

# Numerical Methods for Differential Equations

Copy of e-mail Notification

Your article (1173 ) from Numerical Methods for Differential Equations is available for download

=====

Numerical Methods for Differential Equations Published by John Wiley & Sons, Inc.

Dear Author,

Your page proofs are available in PDF format; please refer to this URL address

<http://kwglobal.co.in/jw/retrieval.aspx>

Login: your e-mail address

Password: ----

The site contains 1 file. You will need to have Adobe Acrobat Reader software to read these files. This is free software and is available for user downloading at <http://www.adobe.com/products/acrobat/readstep.html>. If you have the Notes annotation tool (not contained within Acrobat reader), you can make corrections electronically and return them to Wiley as an e-mail attachment (see the Notes tool instruction sheet). Alternatively, if you would prefer to receive a paper proof by regular mail, please contact Birender/Sundeep(e-mail: [wileysupport@kwglobal.com](mailto:wileysupport@kwglobal.com), phone: +91 (44) 4205-8888 (ext.310)). Be sure to include your article number.

This file contains:

Author Instructions Checklist  
Adobe Acrobat Users - NOTES tool sheet  
Reprint Order form  
Copyright Transfer Agreement  
Return fax form  
A copy of your page proofs for your article

After printing the PDF file, please read the page proofs carefully and:

- 1) indicate changes or corrections in the margin of the page proofs;
- 2) answer all queries (footnotes A,B,C, etc.) on the last page of the PDF proof;
- 3) proofread any tables and equations carefully;
- 4) check that any Greek, especially "mu", has translated correctly.

Special Notes:

1. Figure(s) \_\_\_\_\_ are unacceptable for publication. Please supply good quality hard copy (and/or TIFF or EPS files) when you return your page proofs.

Within 48 hours, please fax or e-mail the following to the address given below:

- 1) original PDF set of page proofs,
- 2) print quality hard copy figures for corrections and/or TIFF or EPS files of figures for correction (if necessary),
- 3) Signed Copyright Transfer Agreement,
- 4) Reprint Order form,
- 5) Return fax form

## Numerical Methods for Differential Equations

Copy of e-mail Notification

Return to:

Production Editor, NUM  
Cadmus Professional Communications  
300 West Chestnut Street  
Ephrata, PA 17522  
U.S.A.  
(See fax number and e-mail address below.)

If you experience technical problems, please contact Birender/Sundeep(e-mail: [wileysupport@kwglobal.com](mailto:wileysupport@kwglobal.com), phone: +91 (44) 4205-8888 (ext.310). Be sure to include your article number.

If you have any questions regarding your article, please contact me. **PLEASE ALWAYS INCLUDE YOUR ARTICLE NO. ( 1173 ) WITH ALL CORRESPONDENCE.**

This e-proof is to be used only for the purpose of returning corrections to the publisher.

Sincerely,

Production Editor, NUM  
Cadmus Professional Communications  
E-mail: [jrnprodnum@cadmus.com](mailto:jrnprodnum@cadmus.com)  
Tel: 717-721-2635  
Fax: 717-738-9478 or 717-738-9479



# WILEY

*Publishers Since 1807*

111 RIVER STREET, HOBOKEN, NJ 07030

**\*\*\*IMMEDIATE RESPONSE REQUIRED\*\*\***

Please follow these instructions to avoid delay of publication.

**READ PROOFS CAREFULLY**

- This will be your only chance to review these proofs.
- Please note that the volume and page numbers shown on the proofs are for position only.

**ANSWER ALL QUERIES ON PROOFS** (Queries for you to answer are attached as the last page of your proof.)

- Mark all corrections directly on the proofs. Note that excessive author alterations may ultimately result in delay of publication and extra costs may be charged to you.

**CHECK FIGURES AND TABLES CAREFULLY** (Color figures will be sent under separate cover.)

- Check size, numbering, and orientation of figures.
- All images in the PDF are downsampled (reduced to lower resolution and file size) to facilitate Internet delivery. These images will appear at higher resolution and sharpness in the printed article.
- Review figure legends to ensure that they are complete.
- Check all tables. Review layout, title, and footnotes.

**COMPLETE REPRINT ORDER FORM**

- Fill out the attached reprint order form. It is important to return the form even if you are not ordering reprints. You may, if you wish, pay for the reprints with a credit card. Reprints will be mailed only after your article appears in print. This is the most opportune time to order reprints. If you wait until after your article comes off press, the reprints will be considerably more expensive.

**RETURN**

- PROOFS**
- REPRINT ORDER FORM**
- CTA (If you have not already signed one)**

**RETURN WITHIN 48 HOURS OF RECEIPT VIA FAX TO 1-717-738-9478 or 717-738-9479**

**QUESTIONS?**

Production Editor, NUM

Phone: 717-721-2635

E-mail: [jrnprodnum@cadmus.com](mailto:jrnprodnum@cadmus.com)

Refer to journal acronym and article production number

## Softproofing for advanced Adobe Acrobat Users – NOTES tool

NOTE: ADOBE READER FROM THE INTERNET DOES NOT CONTAIN THE NOTES TOOL USED IN THIS PROCEDURE.

Acrobat annotation tools can be very useful for indicating changes to the PDF proof of your article. By using Acrobat annotation tools, a full digital pathway can be maintained for your page proofs.

The NOTES annotation tool can be used with either Adobe Acrobat 6.0 or Adobe Acrobat 7.0. Other annotation tools are also available in Acrobat 6.0, but this instruction sheet will concentrate on how to use the NOTES tool. Acrobat Reader, the free Internet download software from Adobe, DOES NOT contain the NOTES tool. In order to softproof using the NOTES tool you must have the full software suite Adobe Acrobat Exchange 6.0 or Adobe Acrobat 7.0 installed on your computer.

### Steps for Softproofing using Adobe Acrobat NOTES tool:

1. Open the PDF page proof of your article using either Adobe Acrobat Exchange 6.0 or Adobe Acrobat 7.0. Proof your article on-screen or print a copy for markup of changes.
2. Go to Edit/Preferences/Commenting (in Acrobat 6.0) or Edit/Preferences/Commenting (in Acrobat 7.0) check “Always use login name for author name” option. Also, set the font size at 9 or 10 point.
3. When you have decided on the corrections to your article, select the NOTES tool from the Acrobat toolbox (Acrobat 6.0) and click to display note text to be changed, or Comments/Add Note (in Acrobat 7.0).
4. Enter your corrections into the NOTES text box window. Be sure to clearly indicate where the correction is to be placed and what text it will effect. If necessary to avoid confusion, you can use your TEXT SELECTION tool to copy the text to be corrected and paste it into the NOTES text box window. At this point, you can type the corrections directly into the NOTES text box window. **DO NOT correct the text by typing directly on the PDF page.**
5. Go through your entire article using the NOTES tool as described in Step 4.
6. When you have completed the corrections to your article, go to Document/Export Comments (in Acrobat 6.0) or Comments/Export Comments (in Acrobat 7.0). Save your NOTES file to a place on your harddrive where you can easily locate it. **Name your NOTES file with the article number assigned to your article in the original softproofing e-mail message.**
7. **When closing your article PDF be sure NOT to save changes to original file.**
8. To make changes to a NOTES file you have exported, simply re-open the original PDF proof file, go to Document/Import Comments and import the NOTES file you saved. Make changes and reexport NOTES file keeping the same file name.
9. When complete, attach your NOTES file to a reply e-mail message. Be sure to include your name, the date, and the title of the journal your article will be printed in.



**John Wiley & Sons, Inc.**  
Publishers Since 1807

**REPRINT BILLING DEPARTMENT • 111 RIVER STREET • HOBOKEN, NJ 07030**  
**PHONE: (201) 748-8789; FAX: (717) 738-9360**

**E-MAIL: reprints @ wiley.com**

**PREPUBLICATION REPRINT ORDER FORM**

**Please complete this form even if you are not ordering reprints.** This form **MUST** be returned with your corrected proofs and original manuscript. Your reprints will be shipped approximately 4 weeks after publication. Reprints ordered after printing are substantially more expensive.

JOURNAL: NUMERICAL METHODS VOLUME \_\_\_\_\_ ISSUE \_\_\_\_\_

TITLE OF MANUSCRIPT \_\_\_\_\_

MS. NO. \_\_\_\_\_ NO. OF PAGES \_\_\_\_\_ AUTHOR(S) \_\_\_\_\_

\*\*25 Reprints will be supplied free of charge

**REPRINTS 7 X 10**

No. of Pages	100 Reprints	200 Reprints	300 Reprints	400 Reprints	500 Reprints
	\$	\$	\$	\$	\$
1-4	193	354	496	627	747
5-8	246	454	642	814	959
9-12	303	557	782	996	1,178
13-16	385	660	927	1,177	1,392
17-20	468	761	1,073	1,353	1,604
21-24	524	864	1,212	1,540	1,815
25-28	591	967	1,357	1,722	2,035
29-32	672	1,068	1,498	1,910	2,254
33-36	739	1,172	1,647	2,091	2,467
37-40	798	1,274	1,788	2,273	2,679

\*\* REPRINTS ARE ONLY AVAILABLE IN LOTS OF 100. IF YOU WISH TO ORDER MORE THAN 500 REPRINTS, PLEASE CONTACT OUR REPRINTS DEPARTMENT AT (201)748-8789 FOR A PRICE QUOTE.

**COVERS**

100 Covers - \$90 • 200 Covers - \$145 • 300 Covers - \$200  
400 Covers - \$255 • 500 Covers - \$325 • Additional 100s - \$65

Please send me \_\_\_\_\_ reprints of the above article at..... \$ \_\_\_\_\_  
 Please send me \_\_\_\_\_ Generic covers of the above journal at..... \$ \_\_\_\_\_  
 Please add appropriate State and Local Tax {Tax Exempt No. \_\_\_\_\_} \$ \_\_\_\_\_  
 Please add 5% Postage and Handling..... \$ \_\_\_\_\_  
**TOTAL AMOUNT OF ORDER\*\*** ..... \$ \_\_\_\_\_

\*\*International orders must be paid in U.S. currency and drawn on a U.S. bank

Please check one:  Check enclosed  Bill me  Credit Card  
 If credit card order, charge to:  American Express  Visa  MasterCard  Discover  
 Credit Card No. \_\_\_\_\_ Signature \_\_\_\_\_ Exp. Date \_\_\_\_\_

**Bill To:** Name \_\_\_\_\_ **Ship To:** Name \_\_\_\_\_  
 Address/Institution \_\_\_\_\_ Address/Institution \_\_\_\_\_

Purchase Order No. \_\_\_\_\_ Phone \_\_\_\_\_ Fax \_\_\_\_\_  
 E-mail: \_\_\_\_\_



111 RIVER STREET, HOBOKEN, NJ 07030

---

Telephone Number:

• Facsimile Number:

To: Production Editor, NUM

Company: Cadmus Professional Communications

Phone: 717-721-2635

Fax: 717-738-9478 or 717-738-9479

From: \_\_\_\_\_

Date: \_\_\_\_\_

Pages including this cover  
page: \_\_\_\_\_

\_\_\_\_\_  
\_\_\_\_\_

Message:

Re:

---

---

# Null-Field Approach for Laplace Problems with Circular Boundaries Using Degenerate Kernels

Jeng-Tzong Chen, Wen-Cheng Shen

Department of Harbor and River Engineering, National Taiwan Ocean University,  
Keelung 20224, Taiwan

Received 26 May 2006; accepted 12 December 2007

Published online in Wiley InterScience (www.interscience.wiley.com).

DOI 10.1002/num.20332

In this article, a semianalytical method for solving the Laplace problems with circular boundaries using the null-field integral equation is proposed. The main gain of using the degenerate kernels is to avoid calculating the principal values. To fully utilize the geometry of circular boundary, degenerate kernels for the fundamental solution and Fourier series for boundary densities are incorporated into the null-field integral equation. An adaptive observer system is considered to fully employ the property of degenerate kernels in the polar coordinates. A linear algebraic system is obtained without boundary discretization. By matching the boundary condition, the unknown coefficients can be determined. The present method can be seen as one kind of semianalytical approaches since error only attributes to the truncated Fourier series. For the eccentric case, vector decomposition technique for the normal and tangential directions is carefully considered in implementing the hypersingular equation in mathematical essence although we transform it to summability to divergent series. The five advantages, well-posed linear algebraic system, principal value free, elimination of boundary-layer effect, exponential convergence, and mesh free, are achieved. Several examples involving infinite, half-plane, and bounded domains with circular boundaries are given to demonstrate the validity of the proposed method. © 2008 Wiley Periodicals, Inc. Numer Methods Partial Differential Eq 00: 000–000, 2008

*Keywords:* degenerate kernel; Fourier series; multiply-connected domain problem; null-field integral equation; semi-analytical approach

## I. INTRODUCTION

The Laplace equation arises in many branches of physics, from which it recruits a wide group of researchers. Temperature in case of steady state heat conduction [1–6], electrostatic potential [7–11], velocity potential in a steady flow of an ideal fluid [12–14], the displacement of an infinite medium under remote uniformly shear [15–19], and the pure torsion of an elastic bar by equilibrated end torques [20, 21] are examples in which the Laplace equation is satisfied. Circular geometries often appear in engineering structures. Although these structures are very simple, the analytical solutions involve special mapping technique or restricted solution representations. Bipolar coordinates was always used to derive the analytical solution for two-holes

*Correspondence to:* Jeng-Tzong Chen, Department of Harbor and River Engineering, National Taiwan Ocean University, Keelung 20224, Taiwan (email: jtchen@mail.ntou.edu.tw)

© 2008 Wiley Periodicals, Inc.

## 2 CHEN AND SHEN

problems [22]. However, conformal mapping or bipolar coordinates is limited to doubly connected regions; most efforts have concentrated on special solution representations. Alternative method has been adopted to solve problems with multiple circular holes [23, 24]. Numerical approaches, e.g. finite difference method (FDM), finite element method (FEM), boundary element method (BEM), and meshfree method, etc. have been used to deal with engineering problems. Among diverse numerical approaches, FEM and BEM have become the popular research tools for engineers. In the past decades, FEM has been widely applied to solve many engineering problems, but one deficiency is that discretizations cost much time to set up the mesh models. Unlike FEM, the discretizations are restricted only to the boundary when using BEM. The main advantage of BEM is one-dimension reduction in mesh generation. For stress concentration problems, BEM can capture the local behavior. It is also ideally suited to the analysis of external problems where domains extend to infinity, since discretizations are confined to the internal boundaries with no need to truncate the domain at a finite distance. There is no doubt that BEM has been appreciated as an alternative numerical method which has been extensively used. Practical engineers and academic researchers paid attention to theoretical study and applications of BEM in the recent decades. Although BEM is recognized as an acceptable tool, some pitfalls still exist, e.g. degenerate scale for potential problems and fictitious frequency for exterior acoustics. Detailed discussions for the pitfalls of BEM can consult with the plenary lecture by Chen et al. [25].

For problems with circular boundaries, the BIEM can be utilized instead of BEM to improve the convergence by introducing Fourier series. The Fourier series expansion is specially tailored to problems with circular geometry. Early attempts to solve problems involving circular boundary using the series expansion were reported by Mogilevskaya et al. [26, 27], Barone and Caulk [2, 28–30], and Bird and Steele [3, 31]. Barone and Caulk explored the use of special boundary integral method for solving Laplace's equation in two-dimensional regions with circular holes. On the basis their idea, the boundary potential and its normal derivative were expressed in a finite series of circular harmonics on each hole. Unlike other approaches, the unknown coefficients in each hole are determined by a new set of integral equations with special kernel functions. However, the explicit equations in [20] were limited to the case when a constant potential is specified on the boundary of each hole. Bird and Steele [3, 31] have adopted the Fourier series for harmonic and biharmonic problems with circular holes. In their numerical results, only six terms of Fourier series on each hole were sufficient to yield error of less than 0.05 percent. More recently, Mogilevskaya and Crouch presented a method for solving problems with randomly distributed circular elastic inclusions with arbitrary properties [27]. They combined the series expansion technique with a direct boundary integral method. However, all of them didn't employ the null-field integral equation and degenerate kernels [32] in the polar coordinates to fully capture the circular boundary to the author's best knowledge although they have employed the Fourier series. The exponential convergence rate was proved in the Kress' book [32] for BIEM by using degenerate kernel and Fourier series. Numerical experiments was performed for the Stokes flow [33].

In the article, we focus on the problems with circular boundaries and possess a semianalytical approach. The comparison between the present approach and conventional BEM is arranged in Table I. A general-purpose program for circular boundaries with different radii and various positions of center is developed. A major benefit of using circular boundaries is that all integrations can be performed analytically. We expand the boundary density along the boundaries of each hole by using Fourier series expansion and employ the null-field integral equation to develop a system of linear algebraic equations. Several examples including multiple circular cavities are demonstrated to check the validity of the present method. Besides, half-plane problem with a circular hole is considered as the special case.

AQ1

## II. PROBLEM STATEMENT AND MATHEMATICAL FORMULATION

Suppose there are  $N$  randomly distributed circular cavities bounded in the domain  $D$  and enclosed with the boundary,  $B_k (k = 0, 1, 2, \dots, N)$  as shown in Fig. 1. We define

F1

$$B = \bigcup_{k=0}^N B_k. \tag{1}$$

In mathematical physics, many engineering problems can be described by the Laplace equation, the governing equation is written below:

$$\nabla^2 u(x) = 0, \quad x \in D, \tag{2}$$

where  $\nabla^2$  is the Laplacian operator,  $u(x)$  is the potential function and  $D$  is the domain of interest. The integral equation for the domain point can be derived from the third Green's identity [34], we have

$$2\pi u(x) = \int_B T(s, x)u(s)dB(s) - \int_B U(s, x)t(s)dB(s), \quad x \in D, \tag{3}$$

$$2\pi \frac{\partial u(x)}{\partial \mathbf{n}_x} = \int_B M(s, x)u(s)dB(s) - \int_B L(s, x)t(s)dB(s), \quad x \in D, \tag{4}$$

where  $s$  and  $x$  are the source and field points, respectively,  $B$  is the boundary,  $\mathbf{n}_x$  denotes the outward normal vector at field point  $x$  (artificially defined, (1,0) is for the  $x$  gradient and (0,1) for the  $y$  gradient on the interior point), and the kernel function

$U(s, x) = \ln r$ , ( $r \equiv |x - s|$ ), is the fundamental solution which satisfies

$$\nabla^2 U(s, x) = 2\pi \delta(x - s), \tag{5}$$

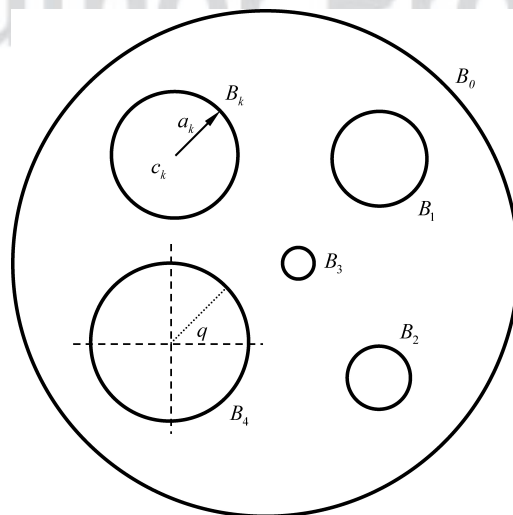


FIG. 1. Problem statements.

#### 4 CHEN AND SHEN

in which  $\delta(x - s)$  denotes the Dirac-delta function. The other kernel functions,  $T(s, x)$ ,  $L(s, x)$  and  $M(s, x)$ , are defined by

$$T(s, x) \equiv \frac{\partial U(s, x)}{\partial \mathbf{n}_s}, L(s, x) \equiv \frac{\partial U(s, x)}{\partial \mathbf{n}_x}, M(s, x) \equiv \frac{\partial^2 U(s, x)}{\partial \mathbf{n}_s \partial \mathbf{n}_x}, \quad (6)$$

where  $\mathbf{n}_s$  is the outward normal vector at the source point  $s$ . By moving the field point to the boundary, the Eqs. (3) and (4) reduce to

$$\pi u(x) = \text{C.P.V.} \int_B T(s, x)u(s)dB(s) - \text{R.P.V} \int_B U(s, x)t(s)dB(s), x \in B, \quad (7)$$

$$\pi \frac{\partial u(x)}{\partial \mathbf{n}_x} = \text{H.P.V.} \int_B M(s, x)u(s)dB(s) - \text{C.P.V} \int_B L(s, x)t(s)dB(s), x \in B, \quad (8)$$

where CPV, RPV, and HPV denote the Cauchy principal value, Riemann principal value, and Hadamard principal value, respectively. Although  $U$ ,  $T$ ,  $L$ , and  $M$  kernels are singular, we can deal with the singular integrals free of principal value sense due to the introduction of degenerate kernel. Once the field point  $x$  locates outside the domain, the null-field integral equation of the direct method in Eqs. (7) and (8) yield

$$0 = \int_B T(s, x)u(s)dB(s) - \int_B U(s, x)t(s)dB(s), x \in D^c \cup B, \quad (9)$$

$$0 = \int_B M(s, x)u(s)dB(s) - \int_B L(s, x)t(s)dB(s), x \in D^c \cup B, \quad (10)$$

where  $D^c$  is the complementary domain. Note that the null-field integral equations are not singular since  $s$  and  $x$  never coincide. Equations (9) and (10) can include the boundary point collocation once the appropriate degenerate kernels are employed. The discontinuity of potentials due to  $T$  and  $L$  kernels automatically appears once the different degenerate expressions for  $T$  and  $L$  kernels are employed for the collocation point inside or outside the circular boundary. Readers can refer to the Appendix of [35].

### III. EXPANSIONS OF FUNDAMENTAL SOLUTION AND BOUNDARY DENSITY

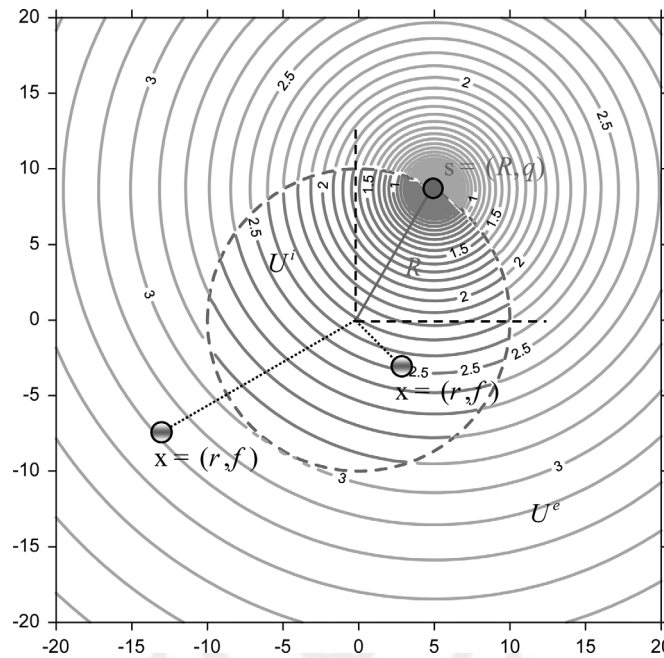
Now, we adopt the mathematical tools, degenerate kernels, and Fourier series for the purpose of analytical study. The combination of degenerate kernels and Fourier series plays the major role in handling problems with circular boundaries.

**Degenerate Kernels for Fundamental Solutions** On the basis of the separable property, the kernel function  $U(s, x)$  can be expanded into separable form by separating the source point and field point in the polar coordinates [36]:

$$U(s, x) = \begin{cases} U^i(R, \theta; \rho, \phi) = \ln R - \sum_{m=1}^{\infty} \frac{1}{m} \left(\frac{\rho}{R}\right)^m \cos m(\theta - \phi), R \geq \rho \\ U^e(R, \theta; \rho, \phi) = \ln \rho - \sum_{m=1}^{\infty} \frac{1}{m} \left(\frac{R}{\rho}\right)^m \cos m(\theta - \phi), \rho > R \end{cases}, \quad (11)$$

where the superscripts “ $i$ ” and “ $e$ ” denote the interior ( $R \geq \rho$ ) and exterior ( $\rho > R$ ) cases, respectively. The origin of the observer system for the degenerate kernel is (0,0). Figure 2 shows

NULL-FIELD APPROACH USING DEGENERATE KERNELS 5



AQ3

FIG. 2. Graph of the separate form of fundamental solution where the source  $s$  located at  $R = 10.0$  and  $\theta = \frac{\pi}{3}$ . [Color figure can be viewed in the online issue, which is available at [www.interscience.wiley.com](http://www.interscience.wiley.com).]

the diagram of degenerate form for fundamental solution where the source point  $s$  located at  $R = 10.0$ ,  $\theta = \pi/3$ . By setting the origin at  $o$  for the observer system, a circle with a radius  $R$  from the origin  $o$  to the source point  $s$  is plotted. If the field point  $x$  is situated inside the circular region, the degenerate kernel belongs to the interior case  $U^i$ ; otherwise, it is the exterior case. After taking the normal derivative with respect to Eq. (11), the  $T(s, x)$  kernel can be derived as

$$T(s, x) = \begin{cases} T^i(R, \theta; \rho, \phi) = \frac{1}{R} + \sum_{m=1}^{\infty} \left( \frac{\rho^m}{R^{m+1}} \right) \cos m(\theta - \phi), R > \rho \\ T^e(R, \theta; \rho, \phi) = - \sum_{m=1}^{\infty} \left( \frac{R^{m-1}}{\rho^m} \right) \cos m(\theta - \phi), \rho > R \end{cases}, \quad (12)$$

and the higher-order kernel functions,  $L(s, x)$  and  $M(s, x)$ , are shown below

$$L(s, x) = \begin{cases} L^i(R, \theta; \rho, \phi) = - \sum_{m=1}^{\infty} \left( \frac{\rho^{m-1}}{R^m} \right) \cos m(\theta - \phi), R > \rho \\ L^e(R, \theta; \rho, \phi) = \frac{1}{\rho} + \sum_{m=1}^{\infty} \left( \frac{R^m}{\rho^{m+1}} \right) \cos m(\theta - \phi), \rho > R \end{cases}, \quad (13)$$

$$M(s, x) = \begin{cases} M^i(R, \theta; \rho, \phi) = \sum_{m=1}^{\infty} \left( \frac{m\rho^{m-1}}{R^{m+1}} \right) \cos m(\theta - \phi), R \geq \rho \\ M^e(R, \theta; \rho, \phi) = \sum_{m=1}^{\infty} \left( \frac{mR^{m-1}}{\rho^{m+1}} \right) \cos m(\theta - \phi), \rho > R \end{cases}. \quad (14)$$

Since the potential resulted from  $T(s, x)$  and  $L(s, x)$  kernels are discontinuous across the boundary, the potentials of  $T(s, x)$  for  $R \rightarrow \rho^+$  and  $R \rightarrow \rho^-$  are different. This is the reason why

6 CHEN AND SHEN

$R = \rho$  is not included in the expression of degenerate kernels for  $T(s, x)$  and  $L(s, x)$  in Eqs. (12) and (13).

**Fourier Series Expansion for Unknown Boundary Densities** We apply the Fourier series expansion to approximate the potential  $u$  and its normal derivative on the boundary

$$u(s_k) = a_0^k + \sum_{n=1}^{\infty} (a_n^k \cos n\theta_k + b_n^k \sin n\theta_k), \quad s_k \in B_k, k = 1, 2, \dots, N, \quad (15)$$

$$t(s_k) = p_0^k + \sum_{n=1}^{\infty} (p_n^k \cos n\theta_k + q_n^k \sin n\theta_k), \quad s_k \in B_k, k = 1, 2, \dots, N, \quad (16)$$

where  $a_n^k, b_n^k, p_n^k$  and  $q_n^k$  ( $n = 0, 1, 2, \dots$ ) are the Fourier coefficients and  $\theta_k$  is the polar angle measured related to the  $x$ -direction.

IV. MATHEMATICAL FORMULATION AND SOLUTION PROCEDURES

A. Adaptive Observer System

In real implementation, the collocation point  $x$  in Eq. (9) can be exactly located on the boundary since the degenerate kernel is introduced. To analytically carry out the  $i$ th circular integral in Eq. (9), we adaptively set the origin of the observer at the center of the  $i$ th circle. Adaptive observer system is chosen to fully employ the property of degenerate kernels. Figure 3(a, b) show the boundary integration for the circular boundaries in the adaptive observer system. The key idea of the present approach is that we employ the null field formulation and we can collocate the point  $x$  on the real boundary due to the introduction of degenerate kernel. It is worthy of note that the origin of the observer system is located at the center of the corresponding integrating circular boundary to entirely utilize the geometry of circular boundary for the expansion of degenerate kernels and boundary densities. The dummy variable in the circular integration is the angle ( $\theta$ ) instead of the radial ordinate ( $R$ ).

B. Linear Algebraic Equation

F3 By moving the null-field point  $x_k$  to the  $k$ th circular boundary in the sense of limit for Eq. (9) in Fig. 3(a), we have

$$0 = \sum_{k=0}^N \int_{B_k} T(s_k, x_j) u_k(s) dB_k(s) - \sum_{k=0}^N \int_{B_k} U(s_k, x_j) t_k(s) dB_k(s), \quad x_j \in D^c. \quad (17)$$

In the real computation, we select the collocation point on the boundary. If the domain is unbounded, the outer boundary  $B_0$  is a circle with an infinite radius. It is noted that the integration path is counterclockwise for the outer circle. Otherwise, it is clockwise. For the  $B_k$  integral of the circular boundary, the kernels of  $U(s, x)$  and  $T(s, x)$  are, respectively, expressed in terms of degenerate kernels of Eqs. (11) and (12), and  $u(s)$  and  $t(s)$  are substituted by using the Fourier series of Eqs. (15) and (16), respectively. In the  $B_k$  integration, we set the origin of the observer system at the center  $c_k$  to fully utilize the degenerate kernels and Fourier series. By collocating the null-field point on the boundary from outside of the domain, a linear algebraic system is obtained

$$[\mathbf{U}]\{\mathbf{t}\} = [\mathbf{T}]\{\mathbf{u}\}, \quad (18)$$

NULL-FIELD APPROACH USING DEGENERATE KERNELS 7

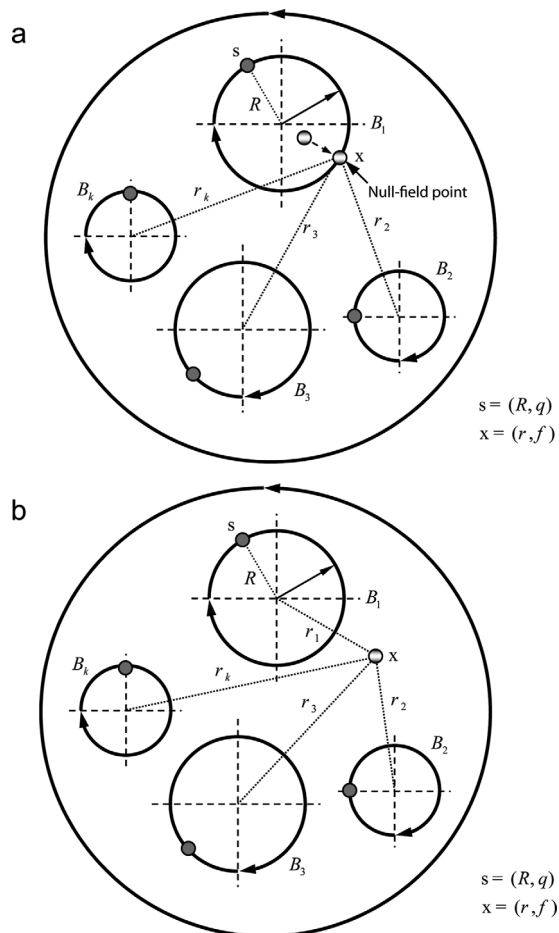


FIG. 3. (a) Sketch of the null-field integral equation in conjunction with the adaptive observer system, (b) sketch of the boundary integral equation for domain point in conjunction with the adaptive observer system. [Color figure can be viewed in the online issue, which is available at [www.interscience.wiley.com](http://www.interscience.wiley.com).]

where  $[U]$  and  $[T]$  are the influence matrices with a dimension of  $N(2M + 1)$  by  $N(2M + 1)$ ,  $\{u\}$ , and  $\{t\}$  denote the column vectors of Fourier coefficients with a dimension of  $N(2M + 1)$  by 1 in which  $M$  indicates the number of truncated terms in Fourier series,  $[U]$ ,  $[T]$ ,  $\{u\}$ , and  $\{t\}$  can be defined as follows:

$$[U] = \begin{bmatrix} U_{00} & U_{01} & \cdots & U_{0N} \\ U_{10} & U_{11} & \cdots & U_{1N} \\ \vdots & \vdots & \ddots & \vdots \\ U_{N0} & U_{N1} & \cdots & U_{NN} \end{bmatrix}, [T] = \begin{bmatrix} T_{00} & T_{01} & \cdots & T_{0N} \\ T_{10} & T_{11} & \cdots & T_{1N} \\ \vdots & \vdots & \ddots & \vdots \\ T_{N0} & T_{N1} & \cdots & T_{NN} \end{bmatrix}, \quad (19)$$

$$\{u\} = \begin{bmatrix} u_0 \\ u_1 \\ u_2 \\ \vdots \\ u_N \end{bmatrix}, \{t\} = \begin{bmatrix} t_0 \\ t_1 \\ t_2 \\ \vdots \\ t_N \end{bmatrix}, \quad (20)$$

8 CHEN AND SHEN

where the vectors  $\{\mathbf{u}_k\}$  and  $\{\mathbf{t}_k\}$  are in the form of  $\{a_0^k a_1^k b_1^k \cdots a_M^k b_M^k\}^T$  and  $\{p_0^k p_1^k q_1^k \cdots p_M^k q_M^k\}^T$ , respectively; the first subscript “ $j$ ” ( $j = 0, 1, 2, \dots, N$ ) in  $[\mathbf{U}_{jk}]$  and  $[\mathbf{T}_{jk}]$  denotes the index of the  $j$ th circle where the collocation point is located and the second subscript “ $k$ ” ( $k = 0, 1, 2, \dots, N$ ) denotes the index of the  $k$ th circle where boundary data  $\{\mathbf{u}_k\}$  or  $\{\mathbf{t}_k\}$  are specified,  $N$  is the number of circular holes in the domain. The coefficient matrix of the linear algebraic system is partitioned into blocks, and each off-diagonal block corresponds to the influence matrices between two different circular cavities. The diagonal blocks are the influence matrices due to itself in each individual hole. After uniformly collocating the point along the  $j$ th circular boundary, the submatrix can be written as

$$[\mathbf{U}_{jk}] = \begin{bmatrix} U_{jk}^{0c}(\phi_1) & U_{jk}^{1c}(\phi_1) & U_{jk}^{1s}(\phi_1) & \cdots & U_{jk}^{Mc}(\phi_1) & U_{jk}^{Ms}(\phi_1) \\ U_{jk}^{0c}(\phi_2) & U_{jk}^{1c}(\phi_2) & U_{jk}^{1s}(\phi_2) & \cdots & U_{jk}^{Mc}(\phi_2) & U_{jk}^{Ms}(\phi_2) \\ U_{jk}^{0c}(\phi_3) & U_{jk}^{1c}(\phi_3) & U_{jk}^{1s}(\phi_3) & \cdots & U_{jk}^{Mc}(\phi_3) & U_{jk}^{Ms}(\phi_3) \\ \vdots & \vdots & \vdots & \ddots & \vdots & \vdots \\ U_{jk}^{0c}(\phi_{2M}) & U_{jk}^{1c}(\phi_{2M}) & U_{jk}^{1s}(\phi_{2M}) & \cdots & U_{jk}^{Mc}(\phi_{2M}) & U_{jk}^{Ms}(\phi_{2M}) \\ U_{jk}^{0c}(\phi_{2M+1}) & U_{jk}^{1c}(\phi_{2M+1}) & U_{jk}^{1s}(\phi_{2M+1}) & \cdots & U_{jk}^{Mc}(\phi_{2M+1}) & U_{jk}^{Ms}(\phi_{2M+1}) \end{bmatrix}, \quad (21)$$

$$[\mathbf{T}_{jk}] = \begin{bmatrix} T_{jk}^{0c}(\phi_1) & T_{jk}^{1c}(\phi_1) & T_{jk}^{1s}(\phi_1) & \cdots & T_{jk}^{Mc}(\phi_1) & T_{jk}^{Ms}(\phi_1) \\ T_{jk}^{0c}(\phi_2) & T_{jk}^{1c}(\phi_2) & T_{jk}^{1s}(\phi_2) & \cdots & T_{jk}^{Mc}(\phi_2) & T_{jk}^{Ms}(\phi_2) \\ T_{jk}^{0c}(\phi_3) & T_{jk}^{1c}(\phi_3) & T_{jk}^{1s}(\phi_3) & \cdots & T_{jk}^{Mc}(\phi_3) & T_{jk}^{Ms}(\phi_3) \\ \vdots & \vdots & \vdots & \ddots & \vdots & \vdots \\ T_{jk}^{0c}(\phi_{2M}) & T_{jk}^{1c}(\phi_{2M}) & T_{jk}^{1s}(\phi_{2M}) & \cdots & T_{jk}^{Mc}(\phi_{2M}) & T_{jk}^{Ms}(\phi_{2M}) \\ T_{jk}^{0c}(\phi_{2M+1}) & T_{jk}^{1c}(\phi_{2M+1}) & T_{jk}^{1s}(\phi_{2M+1}) & \cdots & T_{jk}^{Mc}(\phi_{2M+1}) & T_{jk}^{Ms}(\phi_{2M+1}) \end{bmatrix}. \quad (22)$$

It is noted that the superscript “0s” in Eqs. (21) and (22) disappears since  $\sin \theta = 0$ . The element of  $[\mathbf{U}_{jk}]$  and  $[\mathbf{T}_{jk}]$  are defined respectively as

$$U_{jk}^{nc}(\phi_m) = \int_{B_k} U(s_k, x_m) \cos(n\theta_k) R_k d\theta_k, \quad n = 0, 1, 2, \dots, M, m = 1, 2, \dots, 2M + 1, \quad (23)$$

$$U_{jk}^{ns}(\phi_m) = \int_{B_k} U(s_k, x_m) \sin(n\theta_k) R_k d\theta_k, \quad n = 1, 2, \dots, M, m = 1, 2, \dots, 2M + 1, \quad (24)$$

$$T_{jk}^{nc}(\phi_m) = \int_{B_k} T(s_k, x_m) \cos(n\theta_k) R_k d\theta_k, \quad n = 0, 1, 2, \dots, M, m = 1, 2, \dots, 2M + 1, \quad (25)$$

$$T_{jk}^{ns}(\phi_m) = \int_{B_k} T(s_k, x_m) \sin(n\theta_k) R_k d\theta_k, \quad n = 1, 2, \dots, M, m = 1, 2, \dots, 2M + 1, \quad (26)$$

where  $\phi_m$  is the polar angle of the collocating points  $x_m$  along the boundary.

All the undetermined coefficients are easily determined by using Eq. (18) and the prescribed boundary conditions. Then the unknown boundary values can be determined and the potential at any point can be obtained according to Eq. (3).

**C. Vector Decomposition Technique for the Potential Gradient in the Hyper-Singular Equation**

Equation (4) shows the normal derivative of potential for domain points, special treatment is considered here. Since the hypersingular equation in mathematical essence is also an alternative to deal with the problem of degenerate scale [37–39], potential gradient on the boundary is required to calculate. For the nonconcentric case, special treatment for the normal derivative should be taken care as the source point and field point locate on different circular boundaries. As shown in Fig. 4, the normal direction on the boundary (1, 1') should be superimposed by the radial derivative (3, 3') and angular derivative (4, 4'). We called this treatment “vector decomposition technique.” According to the concept of vector decomposition technique, Eqs. (13) and (14) can be modified as

$$L(s, x) = \begin{cases} L^i(R, \theta; \rho, \phi) = - \sum_{m=1}^{\infty} \left( \frac{\rho^{m-1}}{R^m} \right) \cos m(\theta - \phi) \cos(\zeta - \xi) \\ \quad - \sum_{m=1}^{\infty} \left( \frac{\rho^{m-1}}{R^m} \right) \sin m(\theta - \phi) \cos \left( \frac{\pi}{2} - \zeta + \xi \right), R > \rho \\ L^e(R, \theta; \rho, \phi) = \frac{1}{\rho} + \sum_{m=1}^{\infty} \left( \frac{R^m}{\rho^{m+1}} \right) \cos m(\theta - \phi) \cos(\zeta - \xi) \\ \quad - \sum_{m=1}^{\infty} \left( \frac{R^m}{\rho^{m+1}} \right) \sin m(\theta - \phi) \cos \left( \frac{\pi}{2} - \zeta + \xi \right), \rho > R \end{cases}, \quad (27)$$

$$M(s, x) = \begin{cases} M^i(R, \theta; \rho, \phi) = \sum_{m=1}^{\infty} \left( \frac{m\rho^{m-1}}{R^{m+1}} \right) \cos m(\theta - \phi) \cos(\zeta - \xi) \\ \quad - \sum_{m=1}^{\infty} \left( \frac{m\rho^{m-1}}{R^{m+1}} \right) \sin m(\theta - \phi) \cos \left( \frac{\pi}{2} - \zeta + \xi \right), R \geq \rho \\ M^e(R, \theta; \rho, \phi) = \sum_{m=1}^{\infty} \left( \frac{mR^{m-1}}{\rho^{m+1}} \right) \cos m(\theta - \phi) \cos(\zeta - \xi) \\ \quad - \sum_{m=1}^{\infty} \left( \frac{mR^{m-1}}{\rho^{m+1}} \right) \sin m(\theta - \phi) \cos \left( \frac{\pi}{2} - \zeta + \xi \right), \rho > R \end{cases}, \quad (28)$$

where  $\zeta$  and  $\xi$  are shown in Fig. 4. For the special case, the circles with respect to the same origin of observer, the potential gradient is derived free of special treatment since  $\zeta = \xi$ . F4

**V. ILLUSTRATIVE EXAMPLES AND DISCUSSIONS**

Different branches of engineering applications are given to test our formulation, e.g. steady state heat conduction, electrostatic potential of wires, and flow of an ideal fluid past cylinders. We will introduce the three topics item by item as follows:

**A. Steady State Heat Conduction Problems**

One example derived by Carrier and Pearson [40] and three problems with different boundary conditions found in Caulk’s article [4] are considered.

**Case 1. Eccentric case.** An eccentric case with radii  $a_1$  and  $a_2$  ( $a_1 = 2.5, a_2 = 1.0$ ) is shown in Fig. 5(a). The boundary condition on the inner hole is  $u = 0$  and the potential on the outer circle F5

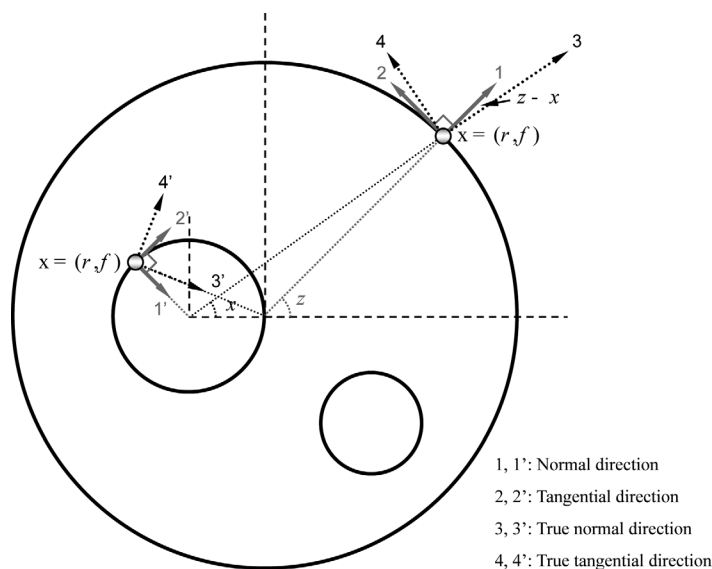


FIG. 4. Vector decomposition for the potential gradient in the hypersingular equation. [Color figure can be viewed in the online issue, which is available at [www.interscience.wiley.com](http://www.interscience.wiley.com).]

is  $u = 1$ . The numerical result is shown in Fig. 5(b). Good agreement is made after comparing the result with the exact solution [10],

$$u(\rho, \phi) = \frac{1}{2 \ln 2} \ln \left[ \frac{16\rho^2 + 1 + 8\rho \cos \phi}{\rho^2 + 16 + 8\rho \cos \phi} \right], \quad (29)$$

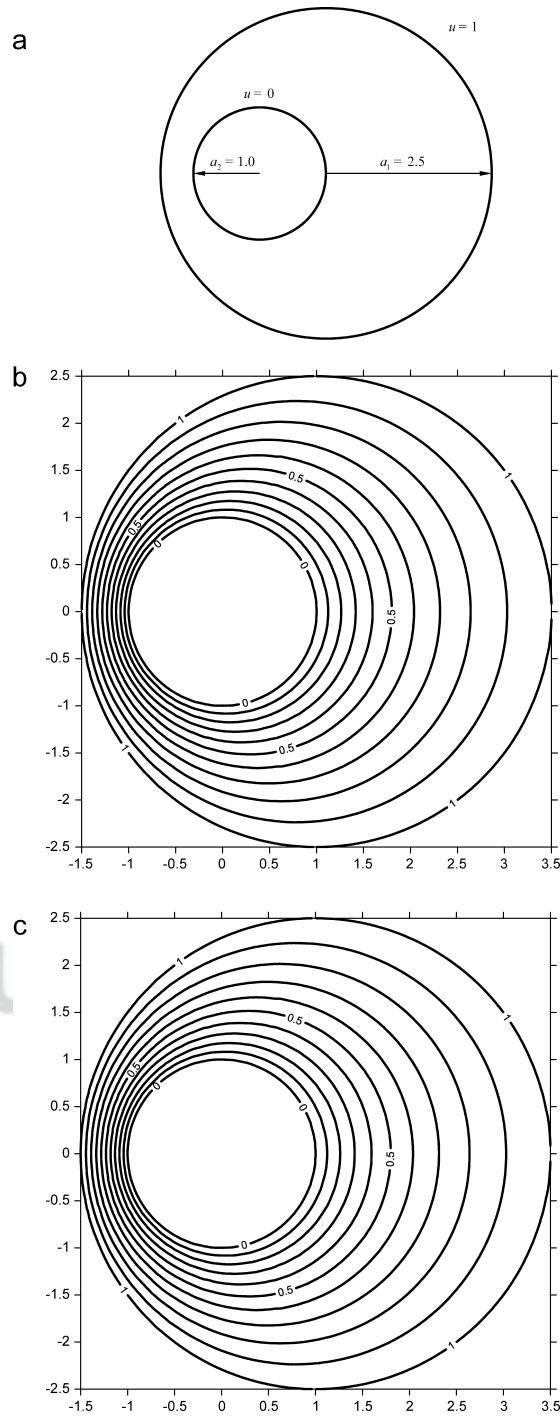
as shown in Fig. 5(c). After determining the Fourier coefficients, we obtain the normal flux on boundaries. The error distribution of flux on the inner boundary using different approaches is shown in Fig. 6. Since error only stems from the truncated terms of Fourier series using the present formulation, the results are better than those using BEM. In addition, the results of present method are also compared with Trefftz method and MFS (Method of Fundamental Solution). Furthermore, we adopted the Parseval theorem to study the convergence rate with different number of terms in Fourier series since the boundary densities are continuous on  $[0, 2\pi]$ . The Parseval's theorem are defined as below

$$\int_0^{2\pi} [f(\theta)]^2 d\theta \doteq 2\pi a_0^2 + \pi \sum_{n=1}^M (a_n^2 + b_n^2). \quad (30)$$

According to Eq. (30), we have the Parseval's sum versus different number of terms in Fourier series for inner circle which are plotted in Fig. 7. Only a few terms of Fourier series are required to yield acceptable results.

**Case 2. Two circular holes in a circle.** A circular region of radius  $R_0$  contains two circular holes which are placed at a distance  $b$  ( $b = 1$ ) from the origin. Both holes have the same radius  $a$  as shown in Fig. 8(a). The radii of the circular holes and the external boundary are  $a = 0.5$  and  $R_0 = 2.0$ . The results are shown in Fig. 8(b). After comparing the result

NULL-FIELD APPROACH USING DEGENERATE KERNELS 11



AQ8

FIG. 5. (a) Laplace problem for the eccentric case, (b) contour plot for the present method (42 collocation points), (c) contour plot for the exact solution [40].

12 CHEN AND SHEN

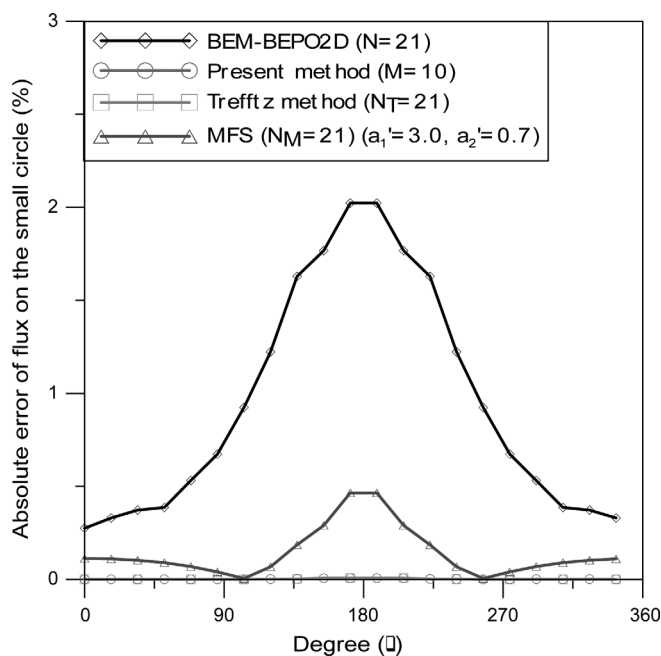


FIG. 6. The relative error distribution for eccentric case using four methods ( $a_1 = 2.5$ , normal scale). [Color figure can be viewed in the online issue, which is available at [www.interscience.wiley.com](http://www.interscience.wiley.com).]

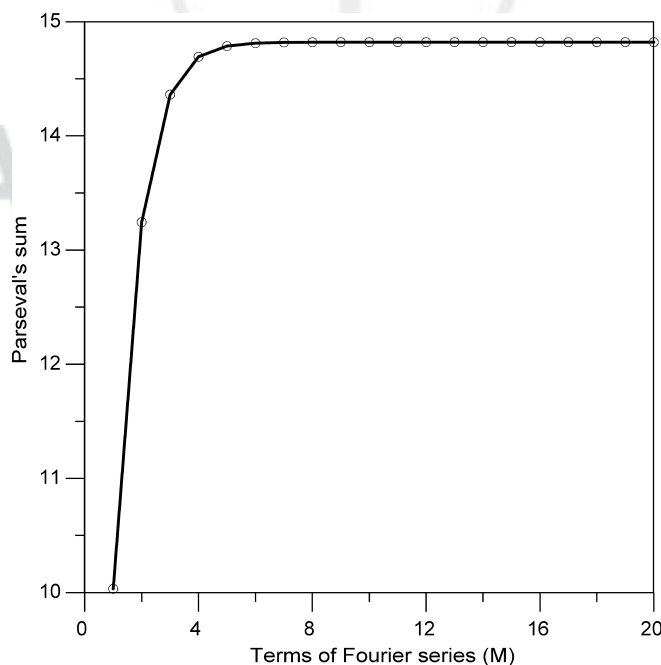


FIG. 7. Parseval's sum for the inner circle.

NULL-FIELD APPROACH USING DEGENERATE KERNELS 13

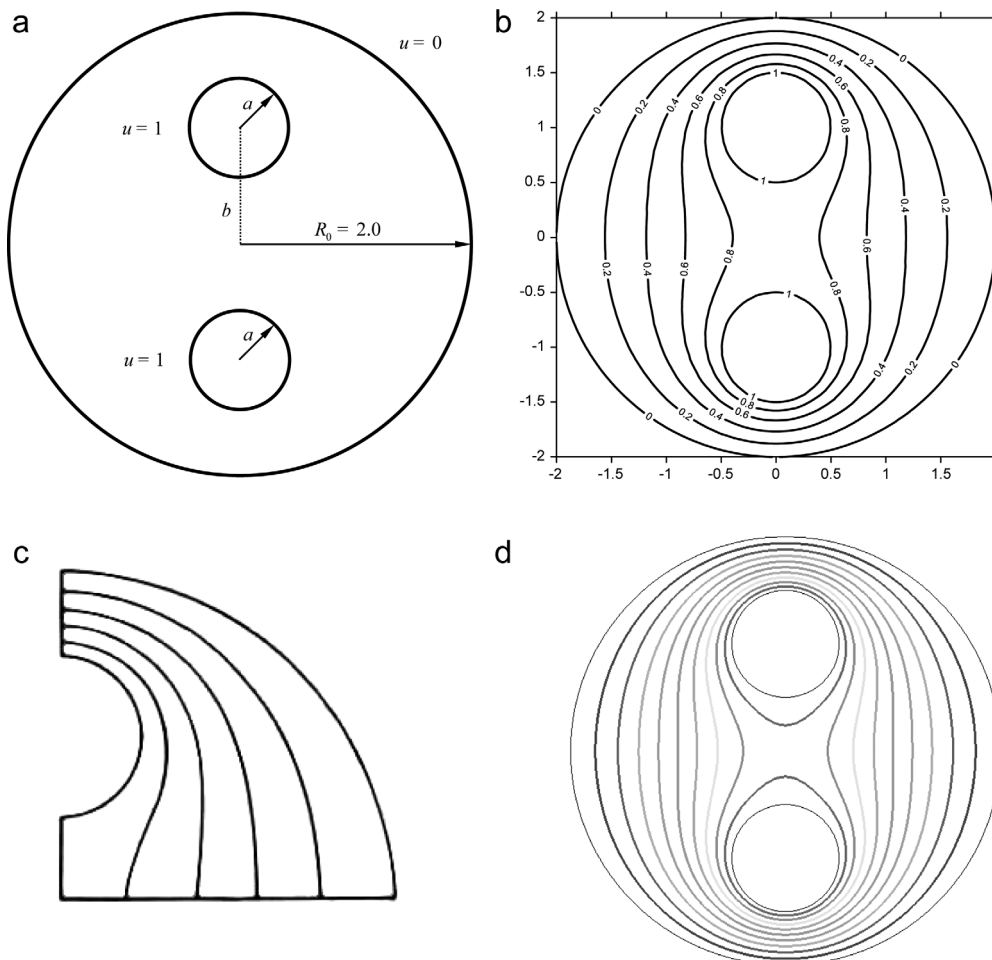


FIG. 8. (a) Problem statements, (b) contour plot for the present method (63 collocation points), (c) quarter part of contour plot for Caulk's data [4], (d) contour plot for FEM-ABAQUS (6502 elements). [Color figure can be viewed in the online issue, which is available at [www.interscience.wiley.com](http://www.interscience.wiley.com).]

with the quarter part of Caulk's result in Fig. 8(c) [4], good agreement is made. ABAQUS shows the result as well as the present procedure with plenty of elements (6502 elements) in Fig. 8(d).

**Case 3. Three circular holes in a circle.** Consider the same region as in the above example, but now add a hole of radius  $c$  at the center. The boundary conditions are different from each other as shown in Fig. 9(a). The radii of the holes are  $a = c = 0.4$  and the distance  $b = 1.2$  from the center of the external boundary. Figure 9(b) shows the numerical results obtained using the present method. The quarter part of the potential by Caulk [4] is shown in Fig. 9(c) for comparison, good agreement is made. Figure 9(d) shows the potential contour using ABAQUS.

F9

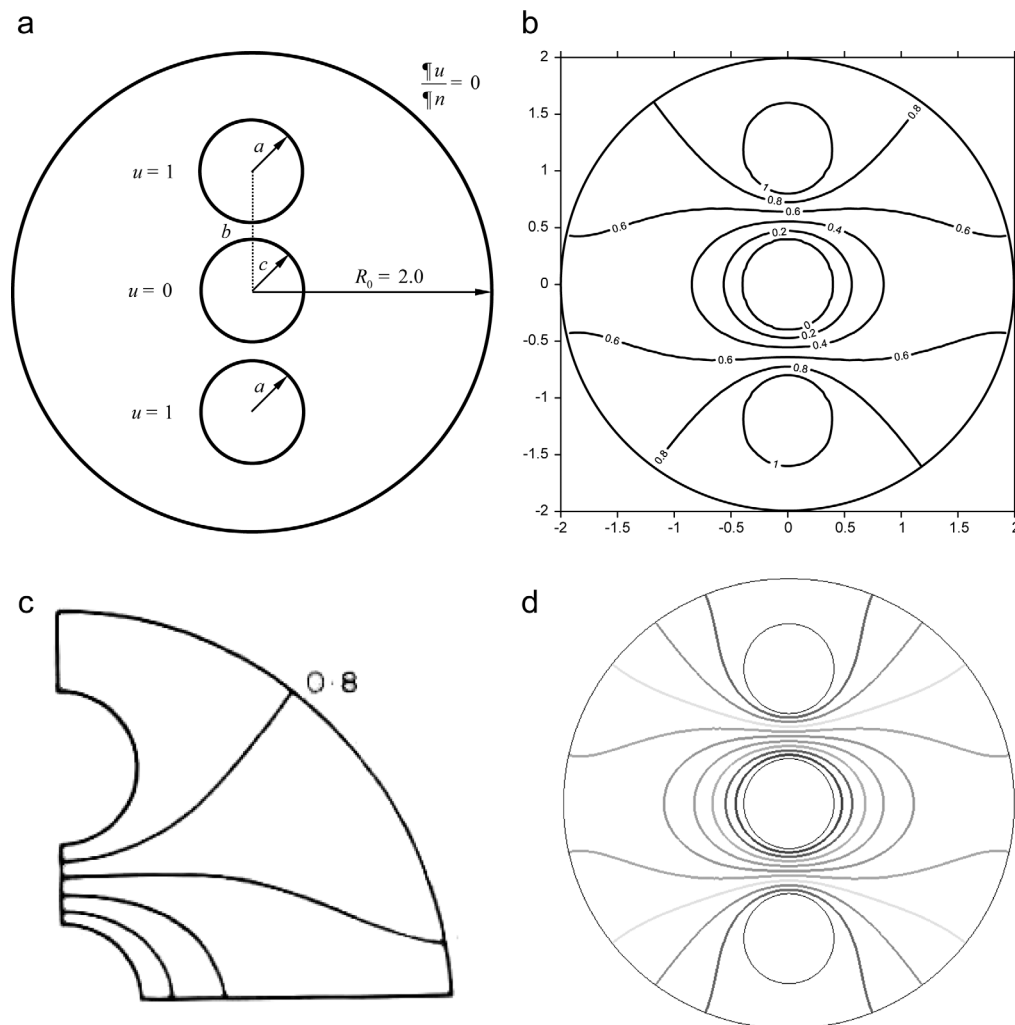


FIG. 9. (a) Problem statements, (b) contour plot for the present method (84 collocation points), (c) quarter part of contour plot for Caulk's data [4], (d) contour plot for FEM-ABAQUS (8050 elements). [Color figure can be viewed in the online issue, which is available at [www.interscience.wiley.com](http://www.interscience.wiley.com).]

### B. Electrostatic Potential of Wires

**Case 1. Electrostatic potential of two parallel cylinders.** The first electrostatic of wires problem reported in [22] is offered to verify the present procedure. Two circular cylindrical conductors of radius  $a$  with centers at distance  $2l$  from each other are charged to potentials 1 and  $-1$ , respectively (see Fig. 10(a)). Numerical results and exact solution by Lebedev et al. are shown in Fig. 10(b, c), respectively.

**Case 2. Hexagonal electrostatic potential.** The other one is a hexagonal electrostatic field of wires which has been solved by Onishi [41]. All the wires have equal radii and the boundary conditions are shown in Fig. 11(a). Figure 11(b) agrees well with Onishi's data as shown in Fig. 11(c).

NULL-FIELD APPROACH USING DEGENERATE KERNELS 15

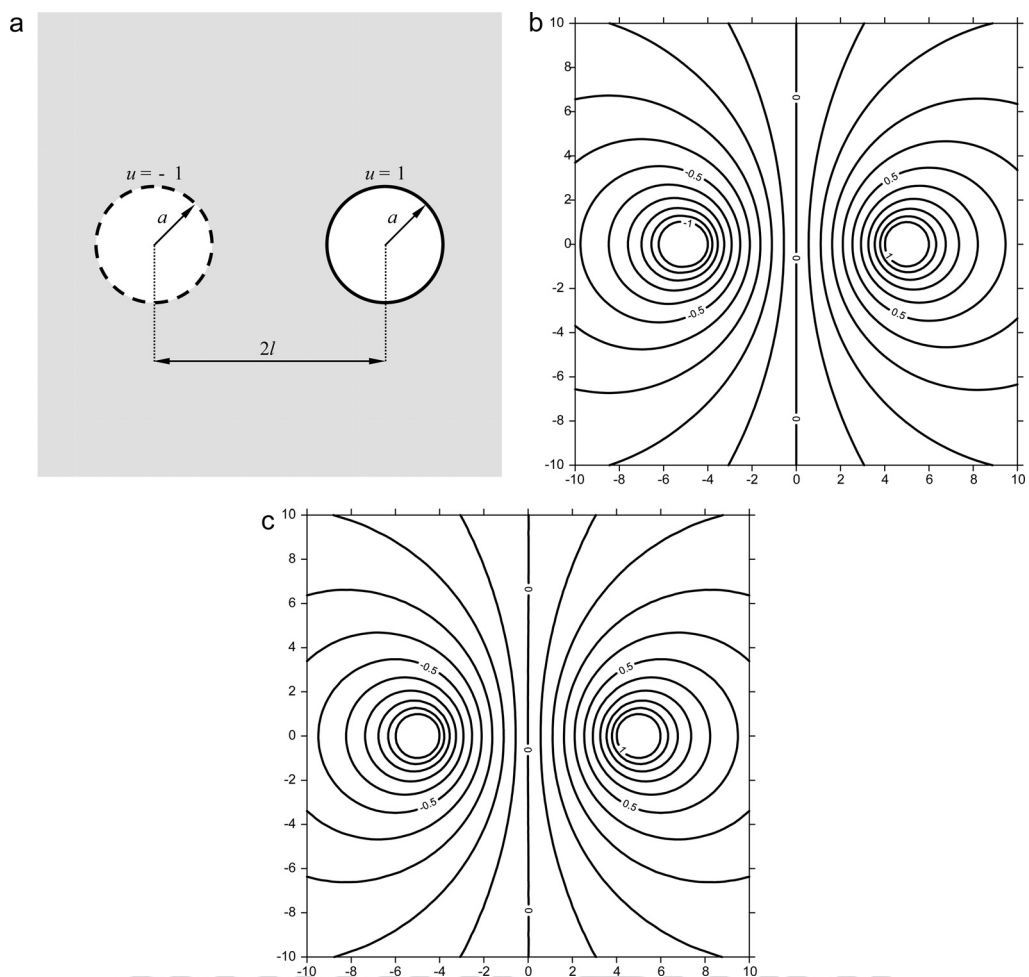


FIG. 10. (a) Two parallel cylinder held positive and negative potentials in an infinite plane, (b) contour plot for the present method (42 collocation points), (c) contour plot for the exact solution [32].

**C. Velocity Potential in a Uniform Flow of an Ideal Fluid**

**Case 1. Uniform flows past a circular cylinder.** Panton [42] have solved the ideal flow about a circular cylinder as shown in Fig. 12(a) with a uniform stream by superposition of a doublet and a stream. The velocity components are computed by complex variables in the cylindrical coordinates as

F12

$$v_r = v^\infty \left( 1 - \frac{a^2}{r^2} \right) \cos \theta, \tag{31}$$

$$v_\theta = -v^\infty \left( 1 + \frac{a^2}{r^2} \right) \sin \theta, \tag{32}$$

where  $v^\infty$  is the velocity of the flow far from the cylinders and  $a$  is the radius of the cylinder. We also revisited the single-cylinder problem by using the proposed formulation. Our results are

16 CHEN AND SHEN

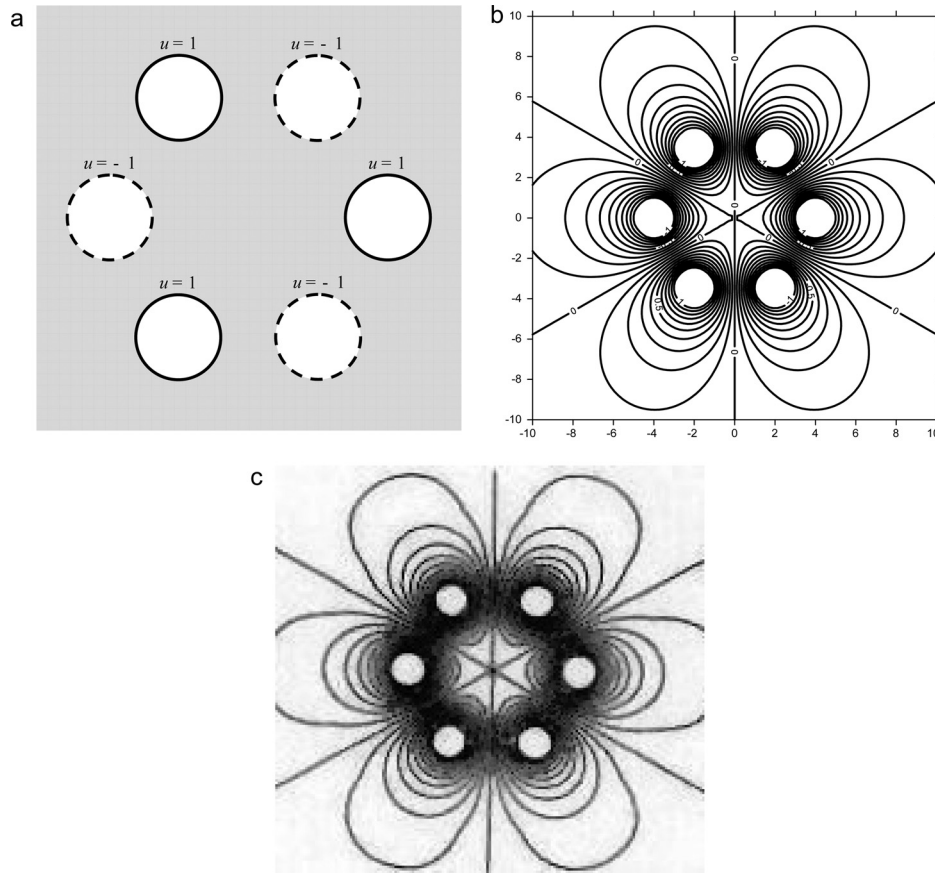


FIG. 11. (a) Hexagonal electrostatic potential in an infinite plane, (b) contour plot for the present method (126 collocation points), (c) contour plot for Onishi's data [44].

consistent with those derived by Panton. The velocity fields with different incident angles  $\gamma$  are shown in Fig. 12(b, c).

**Case 2. Uniform flows past two parallel cylinders.** The other example is referred to [22].  
**F13** Two parallel cylinders of radius  $a$  as shown in Fig. 13(a) with axes a distance  $2l$  apart are placed in a plane-parallel flow of an ideal fluid, making angle  $\gamma$  with the line joining the centers of the cylinders. Find the resulting velocity potential. The analytical solution was derived in the bipolar coordinates by Lebedev et al.

$$\begin{aligned}
 u(\alpha, \beta) = & v^\infty \sqrt{l^2 - a^2} \\
 & \times \left\{ \cos \gamma \left[ \frac{\sin h\alpha}{\cos h\alpha + \cos \beta} + 2 \sum_{n=1}^{\infty} (-1)^n \frac{e^{-n\alpha_0}}{\cos hn\alpha_0} \sin hn\alpha \cos n\beta \right] \right. \\
 & \left. + \sin \gamma \left[ \frac{\sin \beta}{\cos h\alpha + \cos \beta} + 2 \sum_{n=1}^{\infty} (-1)^n \frac{e^{-n\alpha_0}}{\sin hn\alpha_0} \cos hn\alpha \sin n\beta \right] \right\}, \quad (33)
 \end{aligned}$$

NULL-FIELD APPROACH USING DEGENERATE KERNELS 17

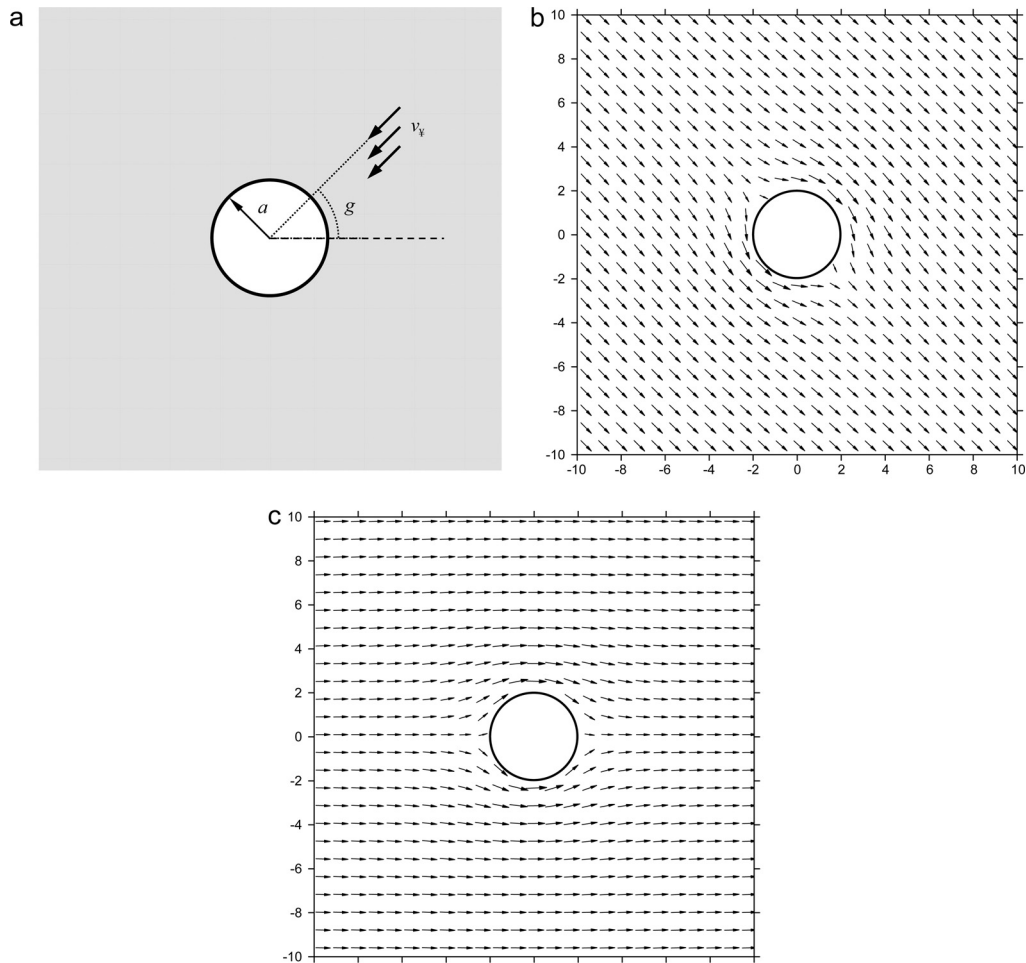


FIG. 12. (a) Flow of an ideal fluid past single cylinder [27], (b) velocity field ( $\gamma = \frac{3\pi}{4}$ ), (c) velocity field ( $\gamma = \pi$ ).

where  $\cos h\alpha_0 = l/a$  and  $v^\infty$  is the velocity of the flow far from the cylinders. The velocity fields are plotted as shown in Fig. 13(b, c) when the angle  $\gamma$  is  $3\pi/4$  and  $\pi$ . For such unbounded problems, FEM is not user friendly and needs truncation of the domain.

**D. Applications to Half-Plane Problems**

Half-plane problems with circular holes [22, 43–45] are considered as the special cases. For the special cases, the image method [19, 23] was employed to satisfy the boundary condition. To avoid the boundary integral along  $B_0$  in Eq. (9) and to satisfy the homogeneous Dirichlet boundary condition, the Green’s function using the image point is obtained

$$U(s; x, x') = \ln |x - s| - \ln |x' - s|, \tag{34}$$

18 CHEN AND SHEN

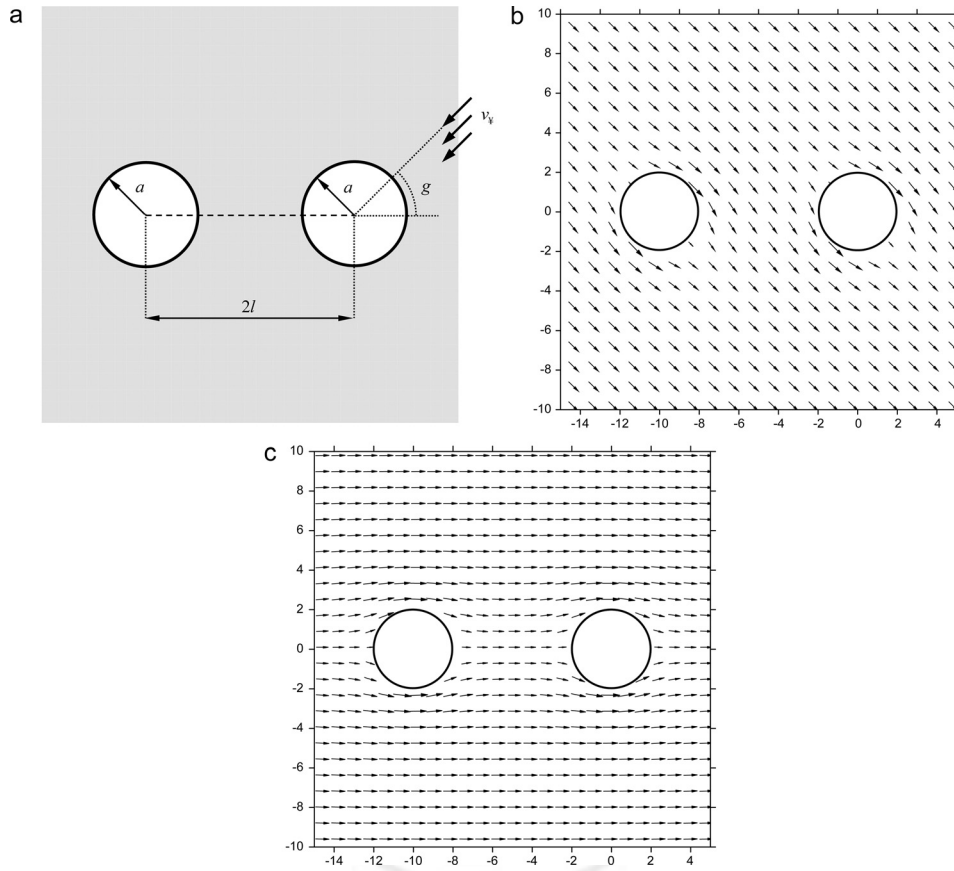


FIG. 13. (a) Flow of an ideal fluid past two parallel cylinders [32], (b) velocity field ( $\gamma = \frac{3\pi}{4}$ ), (c) velocity field ( $\gamma = \pi$ ).

such that

$$U(s; x, x')|_{s \in B_0} = 0. \quad (35)$$

Then, Eqs. (3) and (9) are reduced to

$$2\pi u(x) = \int_B T(s; x, x')u(s)dB(s) - \int_B U(s; x, x')t(s)dB(s), x \in D, \quad (36)$$

$$0 = \int_B T(s; x, x')u(s)dB(s) - \int_B U(s; x, x')t(s)dB(s), x \in D^c, \quad (37)$$

**F14** where  $U(s; x, x')$  denotes the Green's function. On the basis of the Fig. 14, we employ the image concept and obtain

$$U(s, x') = \ln r' = \begin{cases} U^i(R, \theta; \rho', \phi') = \ln R - \sum_{m=1}^{\infty} \frac{1}{m} \left(\frac{\rho'}{R}\right)^m \cos m(\theta - \phi'), R > \rho' \\ U^e(R, \theta; \rho', \phi') = \ln \rho' - \sum_{m=1}^{\infty} \frac{1}{m} \left(\frac{R}{\rho'}\right)^m \cos m(\theta - \phi'), \rho' > R \end{cases}, \quad (38)$$

NULL-FIELD APPROACH USING DEGENERATE KERNELS 19

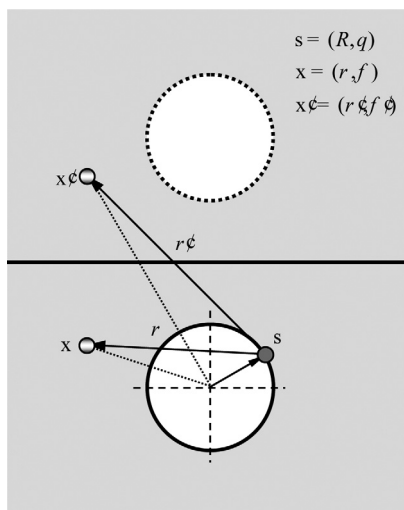


FIG. 14. Considered problem and the auxiliary system. [Color figure can be viewed in the online issue, which is available at www.interscience.wiley.com.]

where  $x' = (\rho', \phi')$  is the image point outside the half-plane domain. The degenerate kernels for the Green's function are

$$\begin{aligned}
 U(s; x, x') &= \ln r - \ln r' \\
 &= \begin{cases} U^i(R, \theta; \rho, \phi, \rho', \phi') = \ln R - \sum_{m=1}^{\infty} \frac{1}{m} \left(\frac{\rho}{R}\right)^m \cos m(\theta - \phi) \\ \quad - \ln \rho' + \sum_{m=1}^{\infty} \frac{1}{m} \left(\frac{R}{\rho'}\right)^m \cos m(\theta - \phi'), \rho' > R \geq \rho \\ U^e(R, \theta; \rho, \phi, \rho', \phi') = \ln \rho - \sum_{m=1}^{\infty} \frac{1}{m} \left(\frac{R}{\rho}\right)^m \cos m(\theta - \phi) \\ \quad - \ln \rho' + \sum_{m=1}^{\infty} \frac{1}{m} \left(\frac{R}{\rho'}\right)^m \cos m(\theta - \phi'), \rho' > \rho > R \end{cases},
 \end{aligned}
 \tag{39}$$

After taking the normal derivative with respect to Eq. (38), the kernel function,  $T(s; x, x')$ , can be derived as

$$T(s; x, x') = \begin{cases} T^i(R, \theta; \rho, \phi, \rho', \phi') = -\frac{1}{R} - \sum_{m=1}^{\infty} \left(\frac{\rho^m}{R^{m+1}}\right) \cos m(\theta - \phi) \\ \quad - \sum_{m=1}^{\infty} \left(\frac{R^{m-1}}{\rho^m}\right) \cos m(\theta - \phi'), \rho' > R > \rho \\ T^e(R, \theta; \rho, \phi, \rho', \phi') = \sum_{m=1}^{\infty} \left(\frac{R^{m-1}}{\rho^m}\right) \cos m(\theta - \phi) \\ \quad - \sum_{m=1}^{\infty} \left(\frac{R^{m-1}}{\rho'^m}\right) \cos m(\theta - \phi'), \rho' > \rho > R \end{cases}.
 \tag{40}$$

First, a steady state heat transfer problem with semicircle removed [46] is considered as shown in Fig. 15(a). After introducing the image concept, we determine the isotherms in the semi-infinite **F15**

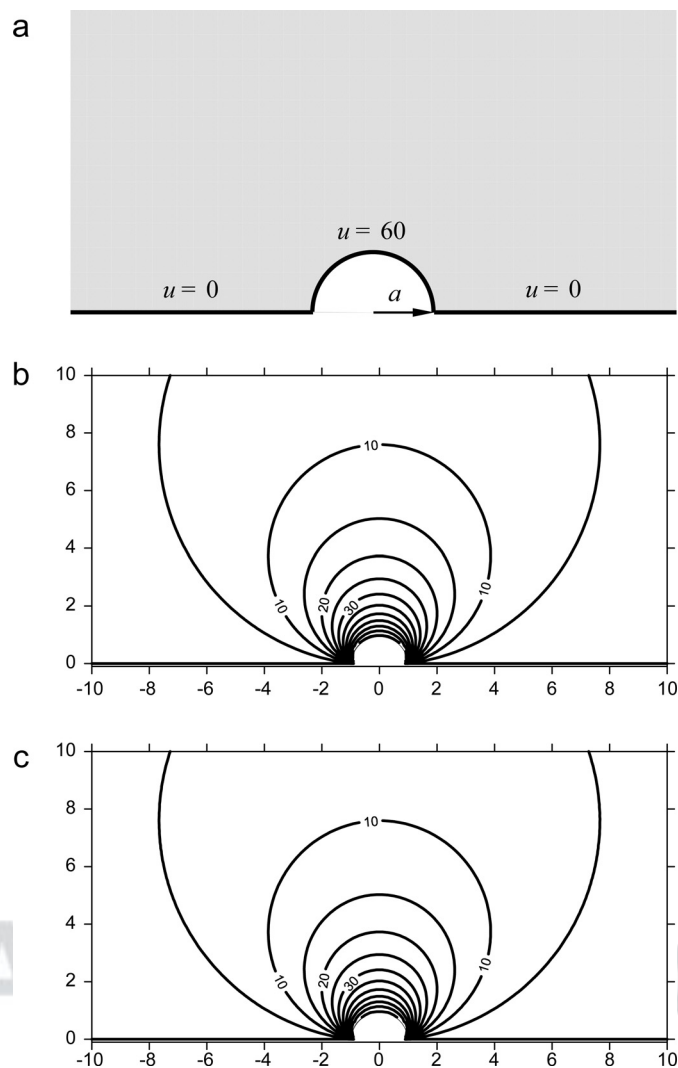


FIG. 15. (a) Steady state heat conduction in a half-plane with semicircle removed, (b) contour plot for the present method (21 collocation points), (c) contour plot for the analytical solution [42].

plane. Figure 15(b, c) show the contour plot for the present method and the analytical solution, respectively. Figure 16(a) give the sketches of the half-plane problems with mixed-type boundary conditions. Figure 16(b) denotes the contour plot of potential using the present method, and Fig. 16(c) is the available exact solutions [22]. The relative error is addressed in Fig. 16(d), and it is found that the results of mixed-type case agree well after comparing them with the exact solution.

## VI. CONCLUDING REMARKS

For the Laplace problems with circular boundaries, we have proposed a special BIEM by using degenerate kernels, null-field integral equation and Fourier series in an adaptive observer system.

NULL-FIELD APPROACH USING DEGENERATE KERNELS 21

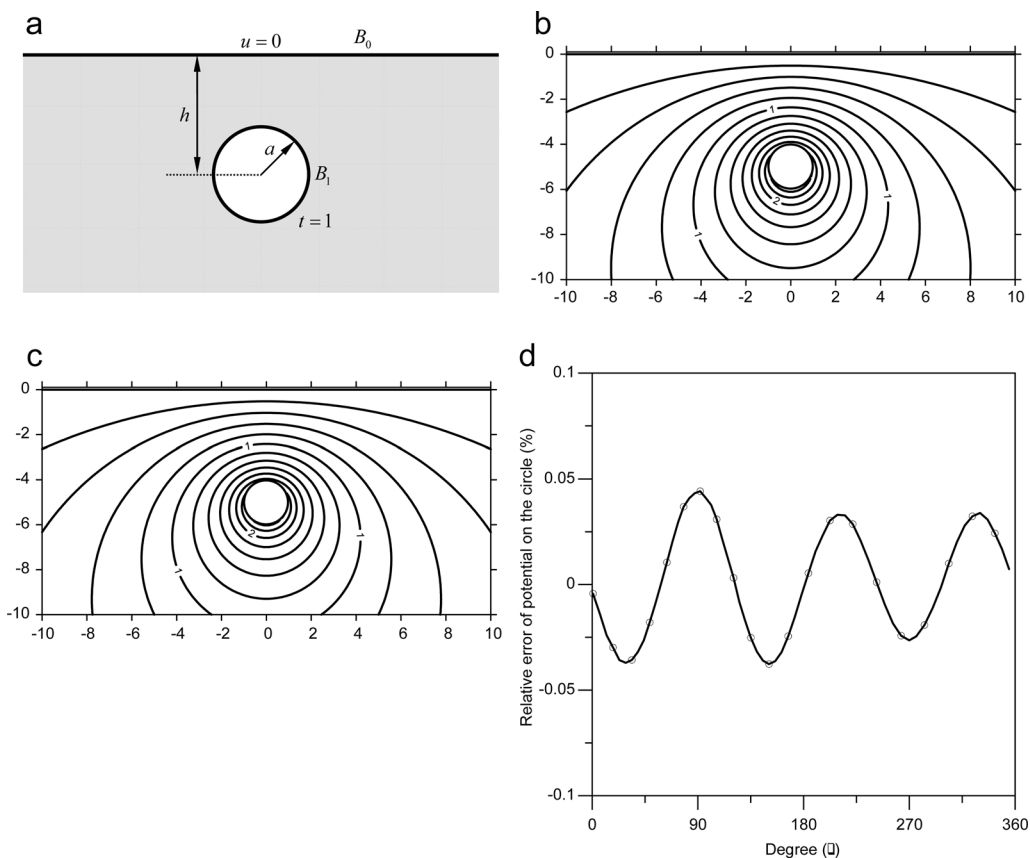


FIG. 16. (a) Half-plane problem subject to mixed-type boundary conditions, (b) contour plot for the present method (21 collocation points), (c) contour plot for the exact solution [32], (d) relative error of boundary potential by using the present method.

The method shows great generality and versatility for the problems with multiple circular holes of arbitrary radii and positions. Numerical results agree very well with the available exact solution and FEM (ABAQUS) and data for only ten terms in Fourier series. Engineering problems with circular boundary which satisfy the Laplace equation can be solved by using the proposed approach in the unified manner.

References

1. M. J. Balcerzak and S. Raynor, Steady state temperature distribution and heat flow in prismatic bars with isothermal boundary conditions, *Int J Heat and Mass Transfer* 3 (1961), 113.
2. M. R. Barone and D. A. Caulk, Optimal arrangement of holes in a two-dimensional heat conductor by a special boundary integral method, *Int J Numer Methods Eng* 18 (1982), 675.
3. M. D. Bird and C. R. Steele, A solution procedure for Laplace’s equation on multiply-connected circular domains, *ASME J Appl Mech* 59 (1992), 398.
4. D. A. Caulk, Analysis of steady heat conduction in regions with circular holes by a special boundary integral method, *IMA J Appl Math* 30 (1983), 231.

AQ4

**22 CHEN AND SHEN**

5. D. A. Caulk, Steady heat conduction from an infinite row of holes in a half-space or a uniform slab, *Int J Heat Mass Transfer* 26 (1983), 1509.
6. K. D. Cole, Fast-converging series for heat conduction in the circular cylinder, *J Eng Math* 49 (2004), 217.
7. H. W. Cheng and L. Greengard, On the numerical evaluation of electrostatic field in dense random dispersions of cylinders, *J Comput Phys* 136 (2002), 629.
8. J. W. Craggs, The determination of capacity for two-dimensional system of cylindrical conductors, *Q J Math* 17 (1946), 131.
9. M. A. Jaswon and G. T. Symm, *Integral equation methods in potential theory and electrostatics*, Academic Press, New York, 1977.
10. D. Palaniappan, Electrostatics of two intersecting conducting cylinders, *Math Comput Modelling* 36 (2002), 821.
11. H. W. Richmond, On the electrostatic field of a plane or circular grating formed of thick rounded bars, *Proc London Math Soc* 22 (1923), 389.
12. R. Barnes and I. Jankovic, Two-dimensional flow through large numbers of circular inhomogeneities, *J Hydrol* 226 (1999), 204.
13. I. Jankovic and R. Barnes, Three-dimensional flow through large numbers of spheroidal inhomogeneities, *J Hydrol* 226 (1999), 224.
14. D. K. Lee, Image singularity system to represent two circular cylinders of different diameter, *ASME J Fluids Eng* 122 (2000), 715.
15. W. T. Ang and I. Kang, A complex variable boundary element method for elliptic partial differential equations in a multiply-connected region, *Int J Comput Math* 75 (2000), 515.
16. S. I. Chou, Stress field around holes in antiplane shear using complex variable boundary element method, *ASME J Appl Mech* 64 (1997), 432.
17. E. Honein, T. Honein, and G. Herrmann, Further aspects of the elastic field for two circular inclusions in antiplane elastostatics, *ASME J Appl Mech* 59 (1992), 774.
18. E. Honein, T. Honein, and G. Herrmann, On two circular inclusions in harmonic problem, *Q Appl Math* 50 (1992), 479.
19. E. Honein, T. Honein, and G. Herrmann, Energetics of two circular inclusions in anti-plane elastostatics, *Int J Solids Struct* 37 (2000), 3667.
20. D. A. Caulk, Analysis of elastic torsion in a bar with circular holes by a special boundary integral method, *ASME J Appl Mech* 50 (1983), 101.
21. C. B. Ling, Torsion of a circular tube with longitudinal circular holes, *Q Appl Math* 5 (1947), 168.
22. N. N. Lebedev, I. P. Skalskaya, and Y. S. Uyand, *Worked problem in applied mathematics*, Dover Publications, New York, 1979.
23. S. X. Gong and S. A. Meguid, Interacting circular inhomogeneities in plane elastostatics, *Acta Mech* 99 (1993), 49.
24. S. X. Gong, Antiplane interaction among multiple circular inclusions, *Mech Res Commun* 22 (1995), 257.
25. J. T. Chen, H.-K. Hong, I. L. Chen, and K. H. Chen, Nonuniqueness and its treatment in the boundary integral equations and boundary element methods, CMC2003 Plenary lecture, Hsin-Chu (2003).
26. S. L. Crouch and S. G. Mogilevskaya, On the use of Somigliana's formula and Fourier series for elasticity problems with circular boundaries, *Int J Numer Methods in Eng* 58 (2003), 537.
27. S. G. Mogilevskaya and S. L. Crouch, A Galerkin boundary integral method for multiple circular elastic inclusions, *Int J Numer Methods Eng* 52 (2001), 1069.

## NULL-FIELD APPROACH USING DEGENERATE KERNELS 23

28. M. R. Barone and D. A. Caulk, Special boundary integral equations for approximate solution of Laplace's equation in two-dimensional regions with circular holes, *Q J Mech and Appl Math* 34 (1981), 265.
29. M. R. Barone and D. A. Caulk, Special boundary integral equations for approximate solution of potential problems in three-dimensional regions with slender cavities of circular cross-section, *IMA J Appl Math* 35 (1985), 311.
30. M. R. Barone and D. A. Caulk, Analysis of liquid metal flow in die casting, *Int J Eng Sci* 38 (2000), 1279.
31. M. D. Bird and C. R. Steele, Separated solution procedure for bending of circular plates with circular holes, *ASME Appl Mech Rev* 44 (1991), 27.
32. R. Kress, *Linear integral equations*, Springer-Verlag, Berlin, 1989.
33. J. T. Chen, C. C. Hsiao, and S. Y. Leu, A new method for Stokes' flow with circular boundaries using degenerate kernel and Fourier series, *Int J Numer Methods Eng*, to appear. AQ5
34. J. T. Chen and H.-K. Hong, Review of dual boundary element methods with emphasis on hypersingular integrals and divergent series, *ASME Appl Mech Rev* 52 (1999), 17.
35. J. T. Chen, W. C. Shen, and P. Y. Chen, Analysis of circular torsion bar with circular holes using null-field approach, *Comput Modelling Eng Sci* 12 (2006), 109.
36. J. T. Chen and Y. P. Chiu, On the pseudo-differential operators in the dual boundary integral equations using degenerate kernels and circulants, *Eng Anal Boundary Elem* 26 (2002), 41.
37. J. T. Chen, J. H. Lin, S. R. Kuo, and Y. P. Chiu, Analytical study and numerical experiments for degenerate scale problems in boundary element method using degenerate kernels and circulants, *Eng Anal Boundary Elem* 25 (2001), 819.
38. J. T. Chen, S. R. Kuo, and J. H. Lin, Analytical study and numerical experiments for degenerate scale problems in the boundary element method for two-dimensional elasticity, *Int J Numer Methods Eng* 54 (2002), 1669.
39. J. T. Chen, C. F. Lee, I. L. Chen, and J. H. Lin, An alternative method for degenerate scale problem in boundary element methods for the two-dimensional Laplace equation, *Eng Anal Boundary Elem* 26 (2002), 559.
40. G. F. Carrier and C. E. Pearson, *Partial differential equations*, Academic Press, New York, 1976.
41. K. Onishi, *Numerical methods for PDE*, Tokyo University Press, Tokyo, 1991.
42. R. L. Panton, *Incompressible flow*, Wiley-Interscience, New York, 1984.
43. C. B. Kooi and A. Verruijt, Interaction of circular holes in an infinite elastic medium, *Tunneling Underground Space Technol* 16 (2001), 59.
44. A. Verruijt, A complex variable solution for a deforming circular tunnel in an elastic half-plane, *Int J Numer Anal Methods Geomech* 21 (1997), 77.
45. A. Verruijt, Deformations of an elastic half plane with a circular cavity, *Int J Solids Struct* 35 (1998), 2795.
46. M. R. Spiegel, *Theory and problems of complex variables with an introduction to conformal mapping and its application*, McGraw-Hill, New York, 1981. AQ6
47. M. D. Greenberg, *Applications of green's function in science and engineering*, Prentice-Hall, New Jersey, 1971. AQ7

## AUTHOR QUERIES

- AQ1:** Please note that Table 1. Citation is provided but the table is not provided in the manuscript.
- AQ2:** Kindly check whether the short title is OK as given.
- AQ3:** Please confirm whether the color figures should be reproduced in color or black and white in the print version. If these color figures must be reproduced in color in the print version, please fill the color charge form immediately and return to Production Editor. Or else, the color figures for your article will appear in color in the online version only.
- AQ4:** Kindly provide complete page range for all the references.
- AQ5:** Kindly update reference 33(if possible).
- AQ6:** Please note that references are renumbered 1–47 to make their citations sequential per journal style.
- AQ7:** Please note that reference 47 (New number) is not cited anywhere in the text. Kindly insert its Citation at an appropriate Please or delete it from the list.
- AQ8:** Kindly check figure 5b & 5c are same. Is it ok?



Author Proof